

Tubeimoside III inhibits lipopolysaccharide-induced inflammatory responses by reprogramming glycolytic metabolism

Wenhua Li¹, Yushi Lin¹, Hongyi Yue¹, Pingyi Wang¹, Yimei Li¹, and Dan Song¹

¹Xizang Minzu University

January 30, 2024

Abstract

OBJECTIVE To investigate how tubeimoside III inhibits lipopolysaccharide(LPS)-induced inflammatory responses by reprogramming glucose metabolism. **METHOD** A mouse model of LPS-induced acute inflammation was constructed, and the protective effect of tubeimoside III against LPS-induced injury was investigated using histochemistry and real-time quantitative PCR. Western blotting, Seahorse extracellular flux analyser assays, and pyruvate content assays were used in LPS-induced RAW264.7 cells to explore how tubeimoside III exerts its anti-inflammatory effects. The potential mechanism was also validated using inhibitors. **RESULTS** Tubeimoside III significantly attenuated the expression of inflammatory cytokines IL-6, IL-1 β , and iNOS in lung and liver tissue homogenates and RAW264.7 cells. This agent inhibited inflammatory cell infiltration in alveoli and prevented necrosis in liver lesions in LPS-treated mice. Extracellular flux analyser assays revealed that tubeimoside III regulated glucose metabolism in RAW264.7 cells. Real-time quantitative PCR and western blot revealed that tubeimoside III had similar effects on the downstream effector molecule of itaconic acid. An inhibitor weakened the inhibitory effect of tubeimoside III on the expression of inflammatory factors. **CONCLUSIONS** Tubeimoside III protects against LPS-induced lung and liver injury by attenuating inflammatory factor secretion and inflammatory cell infiltration, and its mechanism of action involves reprogramming macrophage glucose metabolism and increasing itaconic acid levels.

Tubeimoside III inhibits lipopolysaccharide-induced inflammatory responses by reprogramming glycolytic metabolism

Yushi Lin^{a,b}, Hongyi Yue^{a,b}, Pingyi Wang^{a,b}, Yimei Li^{a,b}, Dan Song^{a,b,*}, Wenhua Li^{a,b,*}

Engineering Research Center of Tibetan Medicine Detection Technology, Ministry of Education, School of Medicine, Xizang Minzu University, Xianyang 712082, Shaanxi, China.

Key Laboratory for Molecular Genetic Mechanisms and Intervention Research on High Altitude Disease of Tibet Autonomous Region, School of Medicine, Xizang Minzu University, Xianyang 712082, Shaanxi, China.

.Yushi Lin and Hongyi Yue have contributed equally to this work and share first authorship.

*. Correspondence to: School of Medicine, Xizang Minzu University, Xianyang 712082, China. E-mail address: xzmylwh@163.com (Wenhua Li), dsong@xzmu.edu.cn (Dan Song).

Abstract

OBJECTIVE

To investigate how tubeimoside III inhibits lipopolysaccharide(LPS)-induced inflammatory responses by reprogramming glucose metabolism.

METHOD

A mouse model of LPS-induced acute inflammation was constructed, and the protective effect of tubeimoside III against LPS-induced injury was investigated using histochemistry and real-time quantitative PCR. Western blotting, Seahorse extracellular flux analyser assays, and pyruvate content assays were used in LPS-induced RAW264.7 cells to explore how tubeimoside III exerts its anti-inflammatory effects. The potential mechanism was also validated using inhibitors.

RESULTS

Tubeimoside III significantly attenuated the expression of inflammatory cytokines IL-6, IL-1 β , and iNOS in lung and liver tissue homogenates and RAW264.7 cells. This agent inhibited inflammatory cell infiltration in alveoli and prevented necrosis in liver lesions in LPS-treated mice. Extracellular flux analyser assays revealed that tubeimoside III regulated glucose metabolism in RAW264.7 cells. Real-time quantitative PCR and western blot revealed that tubeimoside III had similar effects on the downstream effector molecule of itaconic acid. An inhibitor weakened the inhibitory effect of tubeimoside III on the expression of inflammatory factors.

CONCLUSIONS

Tubeimoside III protects against LPS-induced lung and liver injury by attenuating inflammatory factor secretion and inflammatory cell infiltration, and its mechanism of action involves reprogramming macrophage glucose metabolism and increasing itaconic acid levels.

Keyword: Tubeimoside III; Inflammation; Macrophage; Metabolic reprogramming; Itaconic acid; Lipopolysaccharide

Background

Inflammation is a protective response to irritation; excessive or abnormal inflammatory responses exacerbate many acute and chronic diseases. Lipopolysaccharide (LPS) is a bacterial endotoxin that triggers an inflammatory cascade that leads to systemic inflammatory responses. The conventional view is that macrophages activate Toll-like receptor 4, which then activates nuclear factor- κ B (NF- κ B) and the mitogen-activated protein kinase (MAPK) signaling pathways to regulate the expression of downstream inflammatory target genes, including tumor necrosis factor- α (TNF- α), interleukin-1 β (IL-1 β), and IL-6[1, 2].

Bolbostemma paniculatum (Maxim.) Franquet is a member of the Cucurbitaceae family with a long history of medicinal use. The Pharmacopoeia of the People's Republic of China records that it has detoxifying effects, dispersing knots, stopping bleeding, and reducing swelling; it is used to treat canker sores, scrofula, and phlegm toxin[3]. The compounds extracted from *B. paniculatum* include triterpenoids, sterols, alkaloids, anthraquinones, and organic acids. Triterpenoids are abundant active ingredients in *B. paniculatum*, including tubeimosides I, II, and III (Tube)[4]. Tube had anti-inflammatory and anti-swelling effects on ear edema induced by arachidonic acid and 12-O-tetradecanoylphorbol-13-acetate (TPA) in mice, and its effects were more potent than those of tubeimosides I and II[5]. Similar results were reported by Yu et al., who observed that the anti-inflammatory effect of Tube was more potent than those of tubeimosides I and II in a mouse ear edema model[6]. However, to date, the anti-inflammatory mechanism remains unclear. Therefore, in this study, we established an inflammation model in LPS-induced mononuclear macrophages RAW264.7 in mice to investigate Tube's anti-inflammatory effect and molecular mechanisms.

2 Materials and methods

2.1 Animal

Male C57BL/6 mice at 7–10 weeks, weight 20–25 g, were purchased from Xi'an Jiaotong University Experimental Animal Center (originally from the Jackson Laboratory), animal number JAX strain code 000664. The mice were maintained at 24–26 °C, relative humidity of 45%–60%, and a diurnal cycle time of 12:12 hours. They were permitted access to food and water ad libitum. The mice were randomly divided into three groups of ten each, group 1: phosphate-buffered saline (PBS) treatment (Control group); group 2: 10 mg/kg of LPS treatment (LPS group); group 3: 10 mg/kg LPS + 1 mg/kg Tube treatment (Tube group).

The Institutional Animal Care and Use Committee approved the study, and the animal welfare regulations established by the Laboratory Animal Center of Xi'an Jiaotong University were strictly observed.

2.2 Cells

The cell line was derived from the mouse mononuclear macrophage leukemia cell line RAW264.7 (a gift from the Second Affiliated Hospital of Xi'an Jiaotong University). DMEM (Nerzerum, New Zealand) was supplemented with 10% fetal bovine serum Gibco, USA), 100 U/ml penicillin (Amresco, USA), and 100 µg/ml streptomycin (Amresco, USA) and incubated at 37 °C in a 5% CO₂ environment. A Cell Counting Kit-8 (CCK-8, Cat# E606335, Biotech, China) was used to determine the optimal density for cell inoculation.

2.3 Construction of a mouse model of acute inflammation

All mice fasted for 12 hours before the start of the experiment but drank water ad libitum. The Tube group was treated intraperitoneally 3 hours before modeling, while the control and model groups were injected intraperitoneally with an equal volume of saline only. After 3 hours, the model and Tube groups were given LPS (10 mg/kg) intraperitoneally, and the results of hematoxylin and eosin H&E staining judged the success of the modeling. After the injection of each group, mice were placed in cages and allowed to eat and drink ad libitum. The general activity was recorded. Six hours later, the animals were sacrificed, the chest was quickly opened, the organs were removed, and filter paper was used to blot dry surfaces for photography. Then, 0.5 g of tissue samples were homogenized in 1 ml PBS using an ultrasonic disintegrator. The supernatants were centrifuged at 5000 *g* for 5 min at 4 °C and used for subsequent analysis.

2.4 Histopathological analysis

Lung and liver tissues were rapidly dissected from C57BL/6 mice, fixed in 4% paraformaldehyde for 24 h, and embedded in paraffin. Tissue wax blocks were sectioned and stained with H&E (Sangon-Biotech, China). The fixed specimens were stained with H&E after cutting into 4-mm transverse sections using a semi-automatic rotating Thixotrope (Leica Microsystems Trading (Shanghai) Co., Ltd). Pathological changes were recorded under a light microscope (Nikon, Japan).

2.5 Apoptosis detection by flow cytometry

An Annexin V-PE/7-AAD Apoptosis Detection Kit (Yeasen, China) was used to detect apoptosis. Briefly, RAW264.7 cells at 2×10^5 /well were inoculated into six-well plates. After treatment, cells were collected, washed in pre-cooled flow cytometry staining buffer, labeled with Annexin V-PE for 30 min at 4 °C in a dark room, incubated with 7-AAD, and analyzed using flow cytometry (Agilent Technologies, China) and FlowJo software (BD Biosciences, USA).

2.6 NO content measurement

RAW264.7 cells were pretreated with 0/4 µM Tube (MCE, China) for 3 h and stimulated with 1 µg/ml LPS ((Sigma Aldrich, USA) for 0/6/12 h. NO content was measured by mixing 50 µl of medium with Griess reagent [0.1% (w/v) N - (1-naphthyl)ethylenediamine] for 10 min at 37 °C, followed by 50 µl of 1% (w/v) sulfonamide in 5% (v/v) phosphoric acid for 10 min at 37 °C. The absorbance at 540 nm was measured after incubation, and a standard sodium nitrite curve was used to calculate NO concentration.

2.7 Cytokine assay

ELISA kits (Mouse TNF α , Cat# BMS607-3TEN; Mouse IL-6, Cat# BMS603-2; Mouse IL-1 β , Cat#88-7013A-88) were purchased from Thermo Fisher (USA).

2.8 Seahorse extracellular flux analyser assays for ECAR and OCR

The glycolysis rate, spare respiratory capacity, and mitochondrial respiration in RAW264.7 cells were measured using a Seahorse Glycolysis Stress Test Kit (103020-100, Agilent) and a Seahorse Cell Mito Stress Test Kit (103015-100, Agilent) and according to the manufacturer's instructions. Oxygen consumption rate

and extracellular acidification rate were measured on an XFe 96 Seahorse Bioanalyzer (Agilent). Data were analyzed using Wave software (Agilent Technologies).

2.9 Real-time quantitative PCR (qPCR)

Total RNA was isolated using TRIzol reagent (Invitrogen) per the manufacturer’s protocol. RNA was reverse transcribed into cDNA using the SweScript RT I First Strand cDNA Synthesis Kit (With gDNA Remover) (Servicebio, Wuhan, China). qPCR was performed on a QuantStudioTM5 Real-Time PCR instrument (Applied Biosystems, USA) using the SYBR Green PCR Master Mix (Toyobo, Japan) with cDNA template and primers. The primers are displayed in **Table 1**.

Table 1 . Primer sequences for qRT-PCR

Name	Primer sequences (5'-3')
IL-1 β	Forward: AATGACATGCGTGCTCTGGAGAAC
	Reverse: TGGTGAGGTTGCCCGTAGAC
IL-6	Forward: CCAAGAGGTGAGTGCTTCCC
	Reverse: CTGTTGTTTCAGACTCTCTCCCT
iNOS	Forward: GCGCTACAACATCCTGGAGG
	Reverse: CATGATGGTCACATTCTGCTTCTGG
TNF α	Forward: GAGTGACAAGCCTGTAGCCC
	Reverse: GGTGTGGGTGAGGAGCAC
β -actin	Forward: TGATGGTGGGAATGGGTCAG
	Reverse: GGTGTGGTGCCAGATCTTCT
Nfkbiz	Forward: GCTCCGACTCCTCCGATTTC
	Reverse: GAGTTCTTCACGCGAACACC

2.10 Statistical analysis

GraphPad Prism 8 software (San Diego, CA) was used for statistical analysis. All data were expressed as mean \pm standard error of the mean (SEM). A $p < 0.05$ was considered statistically significant; ns ($p > 0.05$) indicates no significant difference between groups.

3 Results

3.1 Effect of Tube on the gross morphology and histology in mouse organs

As shown in **Figure 1**, in the LPS-induced acute inflammation model (see reference[7] for the concentration of LPS), the spleen of the model group was significantly congested with a dark color and blunted rim compared, indicating hyperfunction after LPS treatment. In contrast, the Tube group had less congestion and a relatively lighter color than the model group; however, the overall appearance was similar to that of the control group. This finding suggests that Tube prevents LPS-induced splenic congestion.

The Tube group had significantly fewer erythrocytes in the splenic red marrow, fewer macrophages in the germinal centers, less inflammatory infiltration of the alveolar wall in the lungs, reduced alveolar wall thickness, and reduced structural damage, suggesting that Tube significantly attenuated LPS-induced histomorphological changes in the spleen and lungs, as shown in **Figure 2**. In addition, the LPS sets by looking at Figures 1 and 2 also show that our model construction was successful.

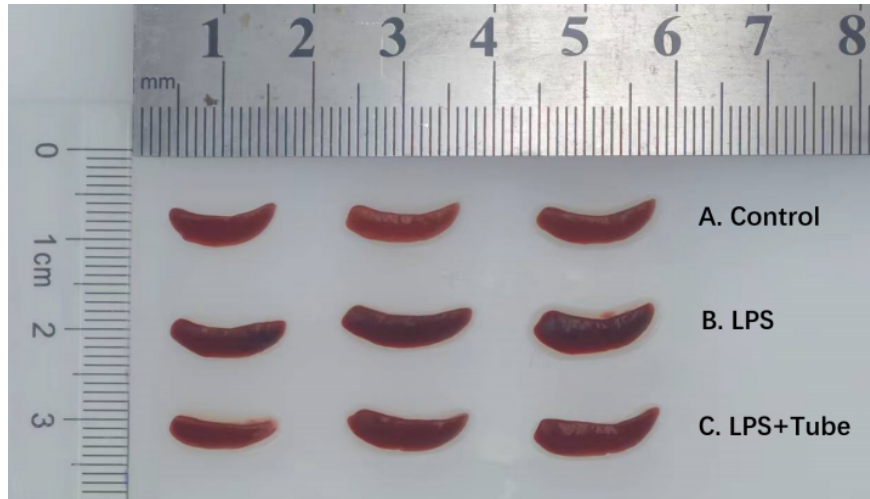
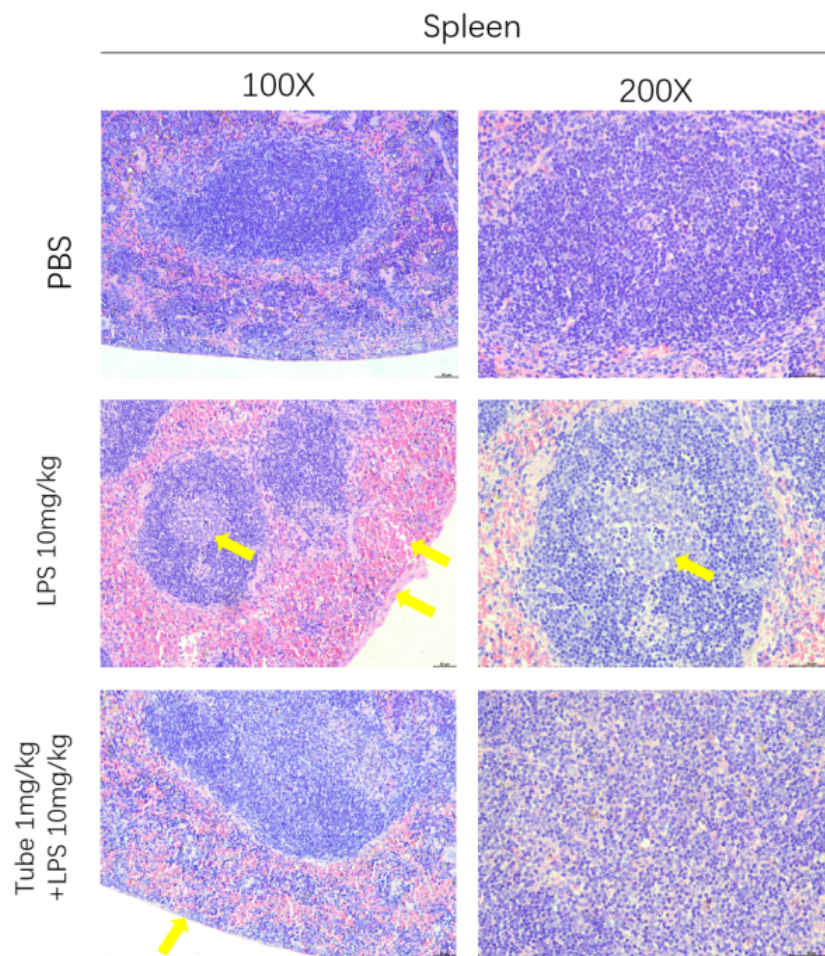


Figure 1. (A) The control group was injected with equal amounts of sterile PBS intraperitoneally. (B) The LPS group was the model group, and 10 mg/kg LPS solution was injected intraperitoneally. (C) The LPS+Tube group was the Tube group, treated with 10 mg/kg LPS solution 3 hours after intraperitoneal injection of 1 mg/kg Tube.



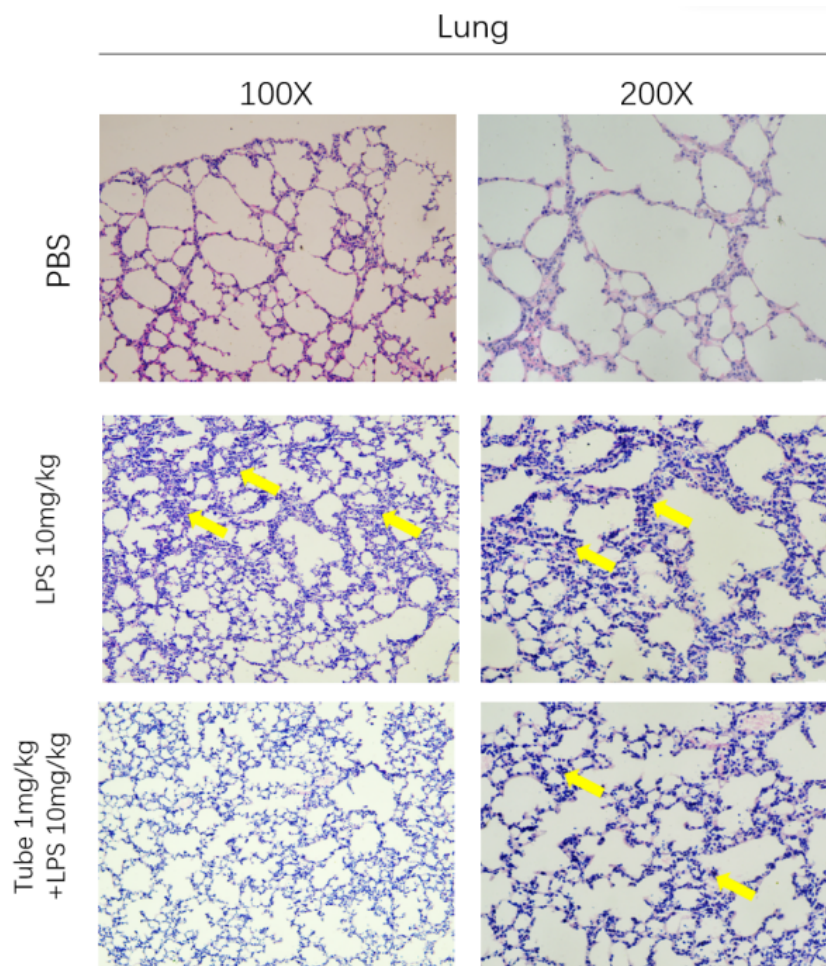


Figure 2. Compared with the control group, the splenic red medulla of the model group was congested with many erythrocytes, the white medulla was reduced in volume, and a large number of macrophages were visible in the germinal center, indicating splenic hyperfunction (shown by the yellow arrow in the left panel). There was thickening of the alveolar wall, increased inflammatory cell infiltration, destruction of alveolar structures, and fusion into large alveoli in the lungs (yellow arrows in the right panel).

3.2 Effect of Tube on mRNA expression of inflammatory factors in mice organs

The mRNA levels of inflammatory factors IL-1 β , IL-6, TNF- α , and iNOS were significantly higher in the liver, spleen, and lung of mice in the model group, indicating that all organs in the model group had different degrees of inflammatory responses (Figure 3A-D). IL-6, and iNOS were significantly lower in the liver, spleen, or lung of mice that were injected intraperitoneally with Tube compared with the model group, as well as IL-1 β in liver and lung. However, the mRNA levels of TNF- α were not significantly different across organs.

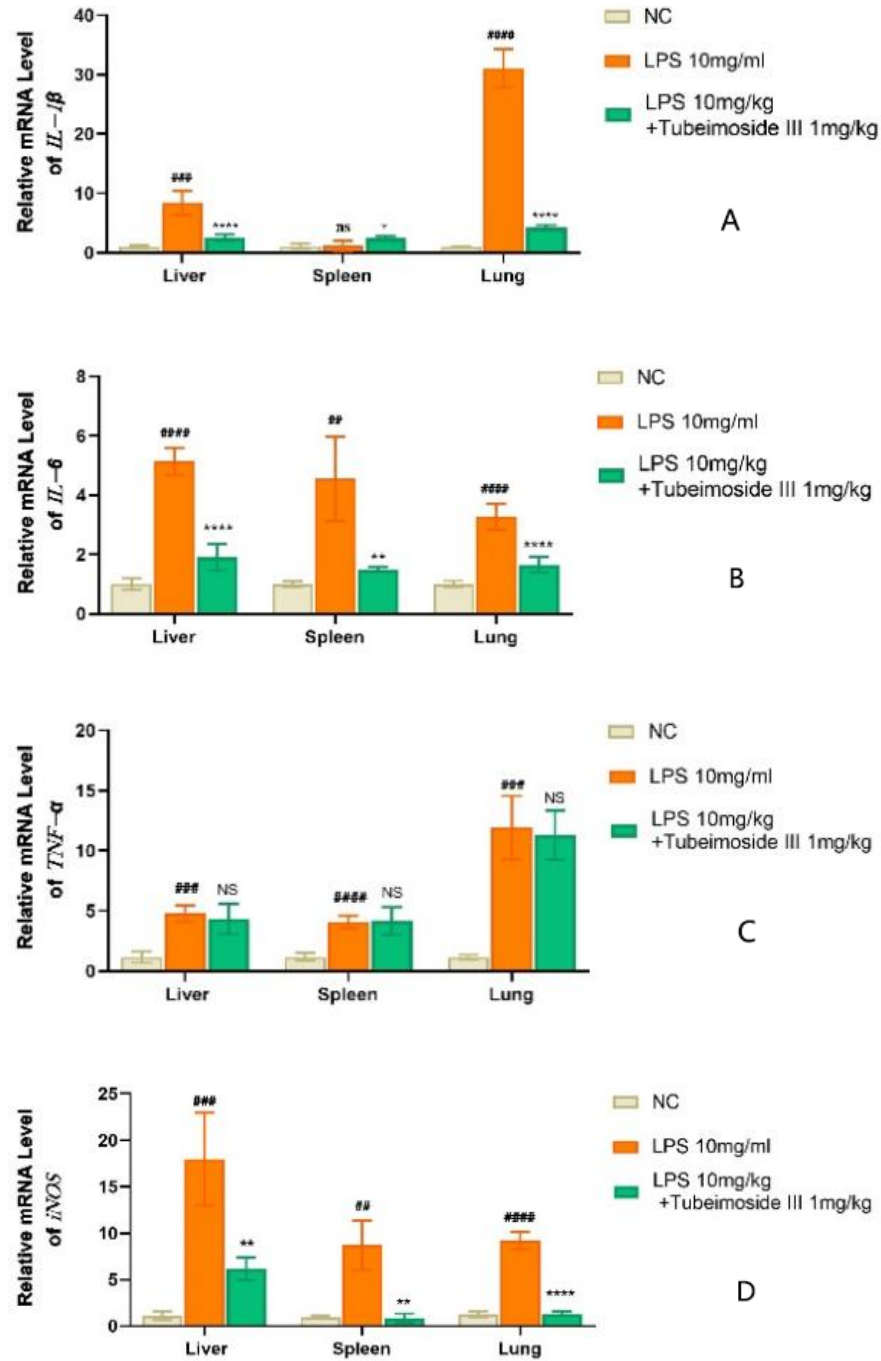


Figure 3. Expression levels of mRNA for inflammatory factors IL-1 β (A), IL-6 (B), TNF- α (C), and iNOS (D) in mouse liver, spleen, and lung. Values are expressed as mean \pm SEM, n = 3. ####P < 0.0001, ###P < 0.001 and ##P < 0.01 vs. NC. ****P < 0.0001, ***P < 0.001, **P < 0.01 and *P < 0.05 vs. LPS.

3.3 Effect of Tube on the viability and apoptosis in RAW264.7 cells

RAW264.7 macrophages in the logarithmic growth phase were resuspended and plated on 12-well plates at 15×10^4 cells per well. The cells were divided into two groups. The first group was treated with various

concentrations of Tube (0, 1, 4, and 7.5 μM), and the second was treated with Tube 4 μM for 0, 3, 6, and 12 hours. Tube had no significant effect on the morphology (**Figure 4**) or apoptosis (**Figure 5**) in RAW264.7 macrophages below 7.5 μM or at 12 h of action.

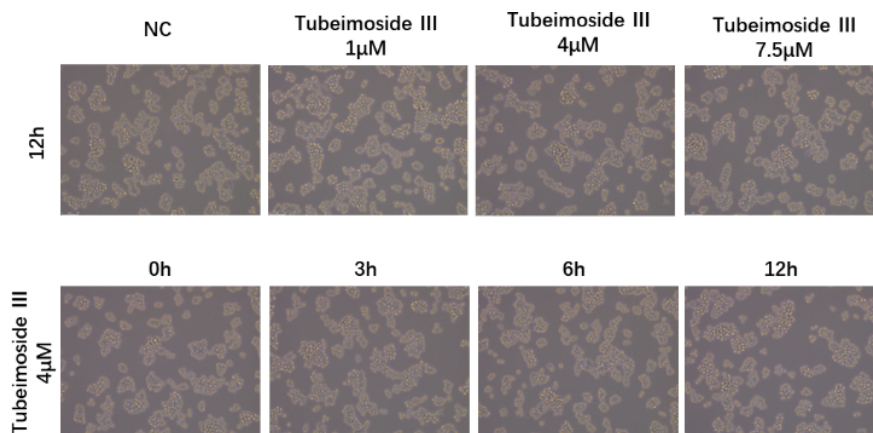


Figure 4. Effect of different concentrations of Tube and 4 μM on the morphology of RAW264.7 macrophages treated for various periods.

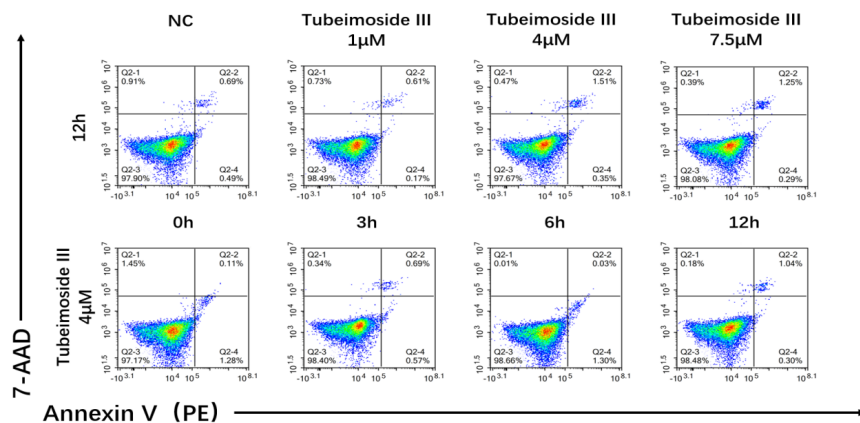


Figure 5. Flow cytometry measurement of apoptosis after treatment of RAW264.7 macrophages with various concentrations of Tube for various durations.

3.4 Effect of Tube on NO and pro-inflammatory cytokines in RAW 264.7 cells

The NO content in the model group increased with increasing LPS treatment time compared with the blank control group (**Figure 6A**), while Tube significantly decreased. Tube significantly inhibited mRNA expression of IL-1 β , IL-6, and iNOS but not of TNF- α in LPS-induced RAW264.7 macrophages (**Figure 6B**).

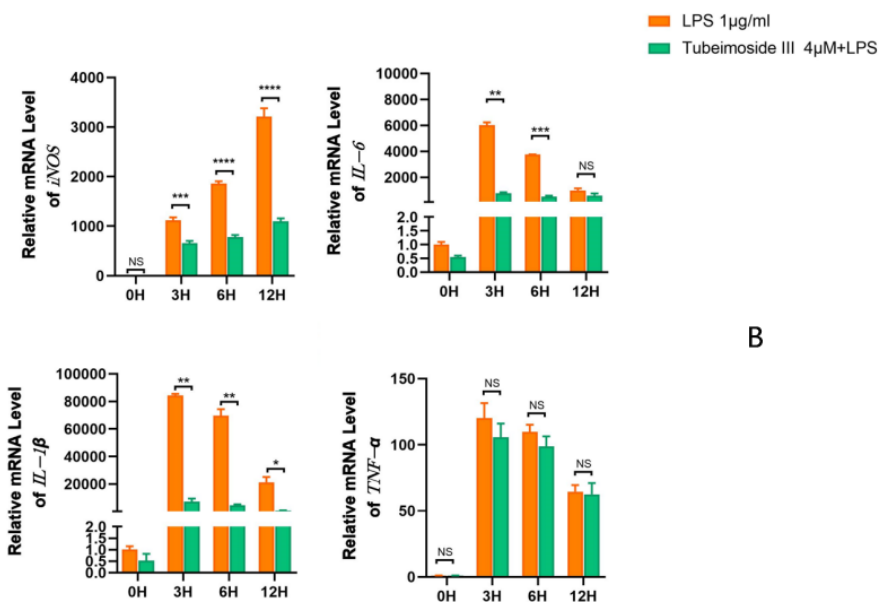
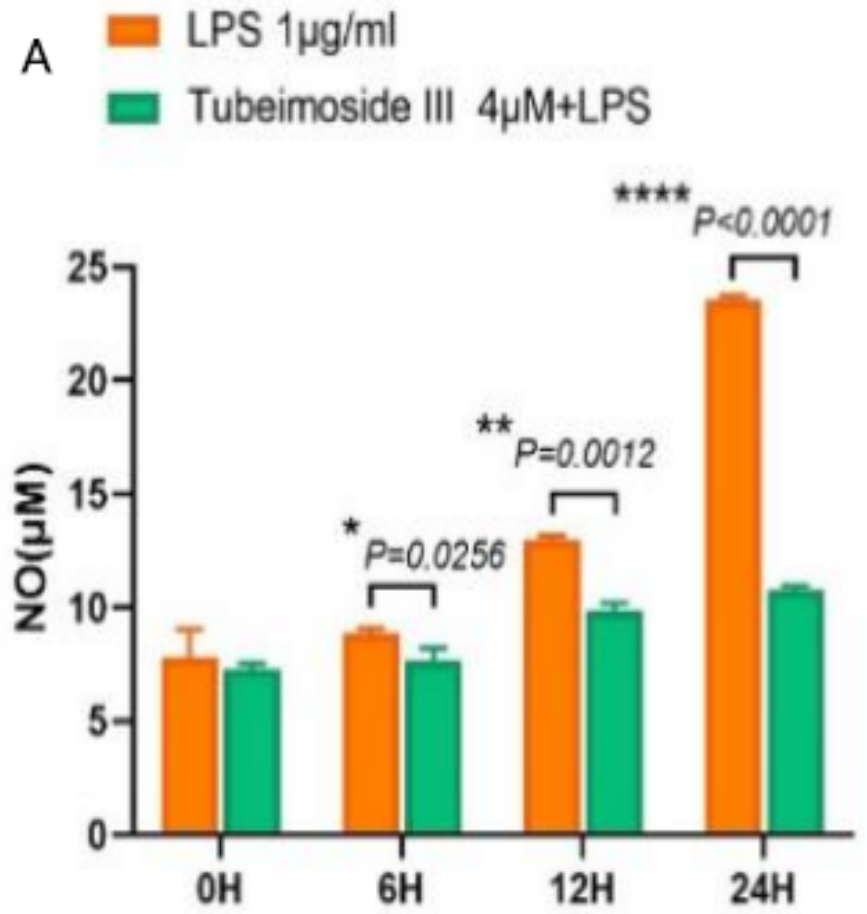


Figure 6. (A) Tube inhibits NO production in LPS-induced RAW264.7 cells. (B) Tube inhibits mRNA levels of iNOS, IL-1 β , and IL-6 but not TNF- α . Values are expressed as mean \pm SEM, and each experiment was repeated three times. ****P < 0.0001, ***P < 0.001, **P < 0.01 and *P < 0.05 vs. LPS.

3.5 Effect of Tube on classical cell signaling pathway-related proteins

The phosphorylation levels of NF- κ B p65, MAPK p38, ERK, and JNK were significantly higher in the model group compared with the blank control group (**Figure 7**). There was no significant difference in the phosphorylation levels of NF- κ B p65, MAPK p38, ERK, or JNK between the Tube and model groups over time, suggesting that the anti-inflammatory effect of Tube may not be significantly associated with the classical NF- κ B signaling pathway.

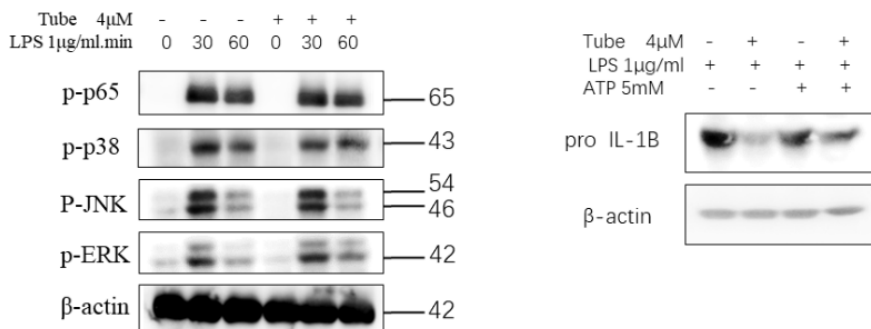
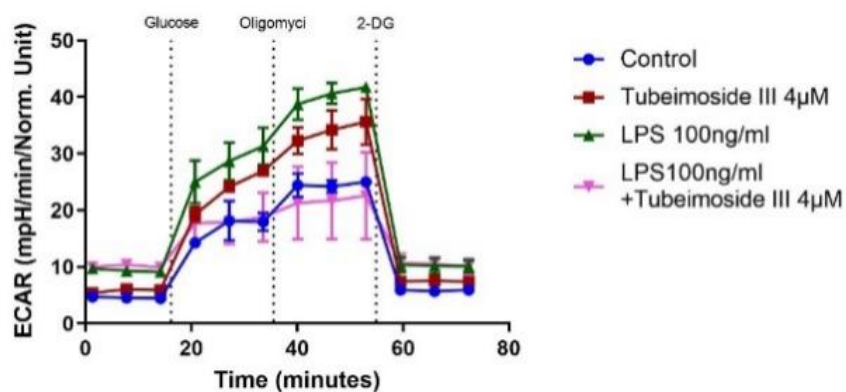


Figure 7. Effect of Tube on LPS-induced NF- κ B p65, MAPK p38, p-ERK, and p-JNK protein phosphorylation levels in RAW264.7 macrophages.

3.6 The effect of Tube on reprogramming sugar metabolism in RAW 264.7 cells

Tube inhibited LPS-induced glycolysis in RAW264.7 macrophages (**Figure 8**) and reduced basal and maximal respiration (**Figure 9**). This finding suggests that Tube inhibits glycolysis in RAW264.7 macrophages at the level of mitochondrial oxidative phosphorylation. The transcript levels of critical glycolytic rate-limiting enzyme genes were measured using RT-PCR. Tube increased the transcript levels of GLUT1, PFKFB3, and hexokinase 2 (HK2), while inhibiting the transcript levels of LDHA (**Figure 10**). Pyruvate content in RAW264.7 macrophages increased with the application Tube (**Figure 11**).



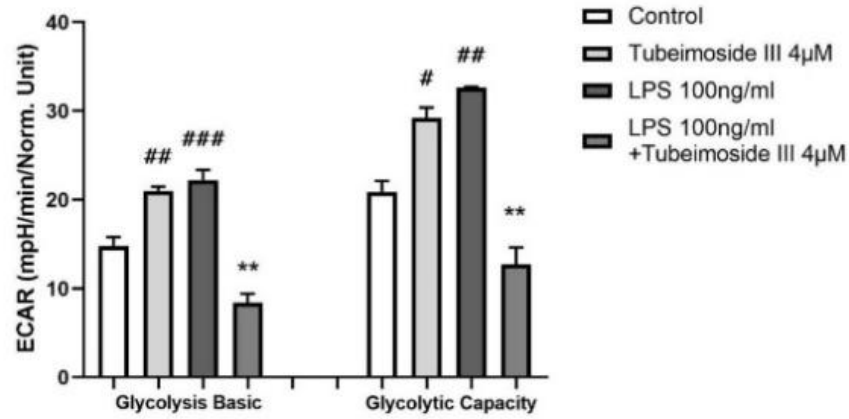


Figure 8. Effect of Tube on the extracellular acidification rate of RAW264.7 macrophages. Compared with the blank control group, the extracellular acidification rate was significantly greater in the LPS model group, and the basal glycolytic capacity and maximum glycolytic capacity were both significantly higher ($##P < 0.01$, $###P < 0.001$). Compared with the LPS group, the basal glycolytic capacity and the maximum glycolytic capacity of cells in the Tube+LPS group were significantly lower ($**P < 0.01$). Values are expressed as mean \pm SEM, and each experiment was repeated three times.

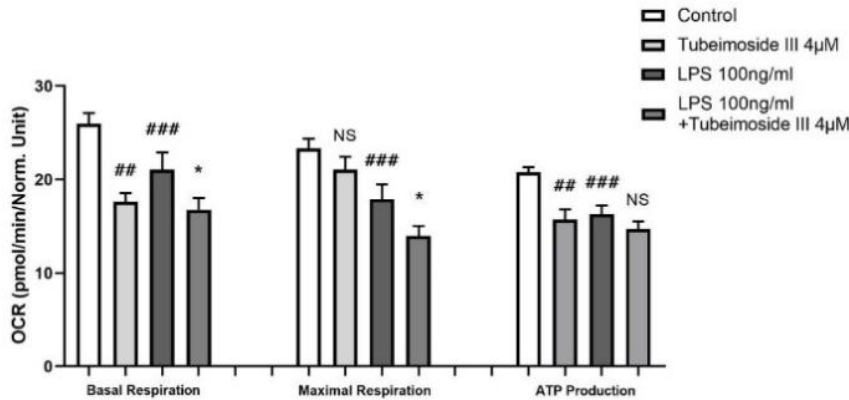
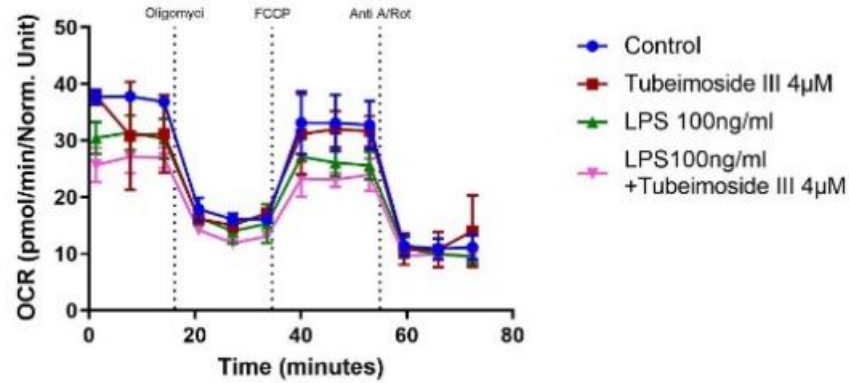


Figure 9. Effect of Tube on the oxygen consumption in RAW264.7 macrophages. Compared with the blank control group, basal respiration, maximum respiration, and ATP production were significantly lower in the LPS model group (### $P < 0.001$). Compared with the LPS group, the basal respiration and maximum respiration of cells in the Tube+LPS group were lower ($*P < 0.05$). Values are expressed as mean \pm SEM, and each experiment was repeated three times.

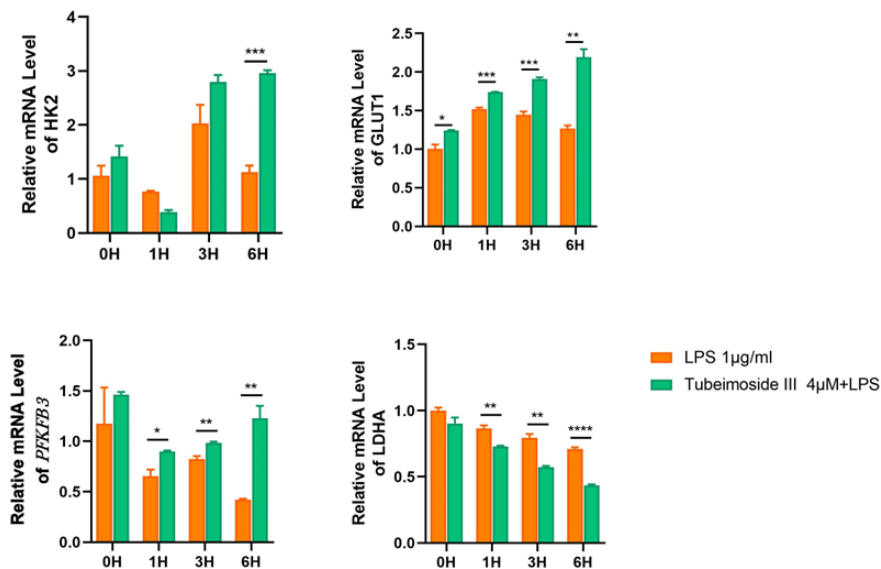


Figure 10. Effect of Tube on mRNA expression levels of genes for rate-limiting molecules of glycolysis in RAW264.7 macrophages. The mRNA expression levels of GLUT1, PFKFB3, and HK2 were higher in the Tube group than the LPS model group at all intervals ($*P < 0.05$, $**P < 0.01$, $***P < 0.001$), while the mRNA expression levels of LDHA, a critical enzyme for lactate production, were significantly lower ($**P < 0.01$, $****P < 0.0001$). Values are expressed as mean \pm SEM, and each experiment was repeated three times.

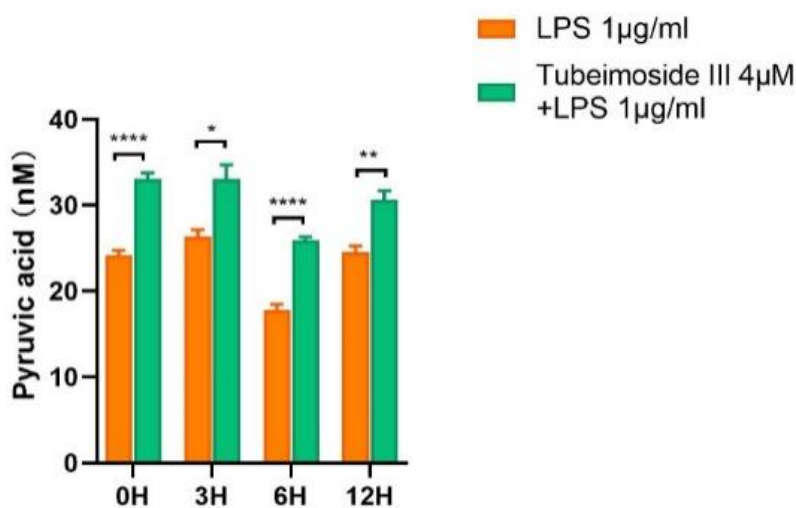


Figure 11. Pyruvate content was more significant in the Tube group than in the LPS model group at all intervals ($*P < 0.05$, $**P < 0.01$, $***P < 0.001$, $****P < 0.0001$), indicating that Tube increased the LPS-induced pyruvate

content in RAW264.7 macrophages. Values are expressed as mean \pm SEM, and each experiment was repeated three times.

3.7 Effect of Tube on the expression level of downstream effector molecules of itaconic acid

We used RT-PCR to measure the expression of downstream effector molecules of itaconic acid, including Nfkbiz, Nrf2, NQO1, HO-1, GCLM, JAK1, STAT6, TET2, and IL-1 α [8-12]. Τη ρεσυλτς αρε σηωων νΦιγυρε 12 .

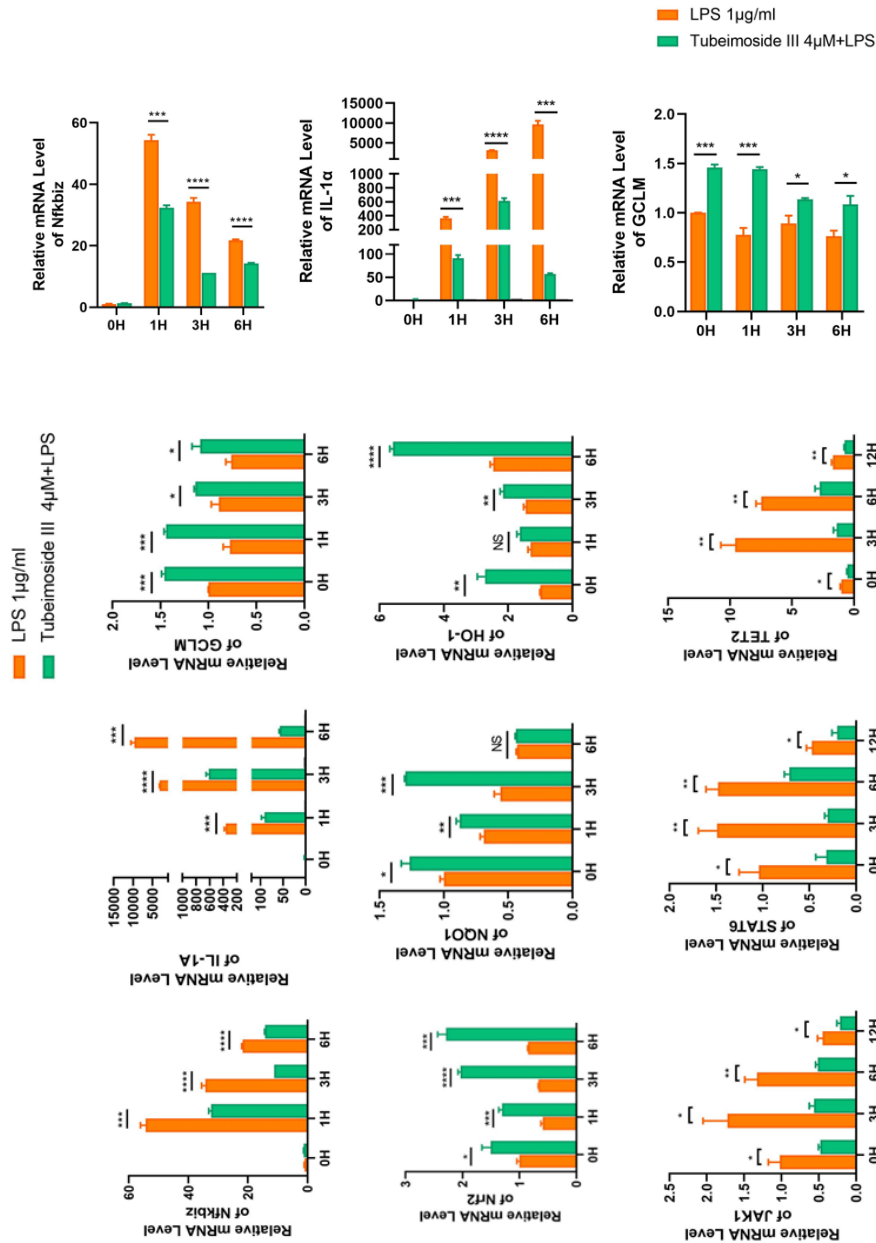


Figure 12. Compared with the LPS model group at each period, the mRNA levels of Nfkbiz (the transcriptional counterpart sequence of I κ B ζ) and its downstream molecule IL-1 α were significantly lower in the Tube group. The mRNA levels of Nrf2, NQO1, HO-1, and GCLM were significantly higher, while the JAK1,

STAT6, and TET2 mRNA levels were significantly lower. *P < 0.05, **P < 0.01, ***P < 0.001, ****P < 0.0001. Values are expressed as mean ± SEM, and each experiment was repeated three times.

3.8 Εμφερεστ οφ Τυβε ον της εξπρεσσιον οφ ΙκΒζ (IκBζ) πρωτειν ω ΡΑΩ 264.7 ρελλς

We measured the changes of ATF3 and IκBζ protein levels in LPS-treated RAW264.7 macrophages by western blot (**Figure 13**). Compared with the LPS model group, ATF3 protein levels were significantly higher, and IκBζ protein levels were significantly lower in the Tube group, regardless of whether LPS was added for one or more hours. These findings suggest that Tube increased the expression of ATF3 and inhibited the expression of IκBζ protein, consistent with the RT-PCR experiment described above.

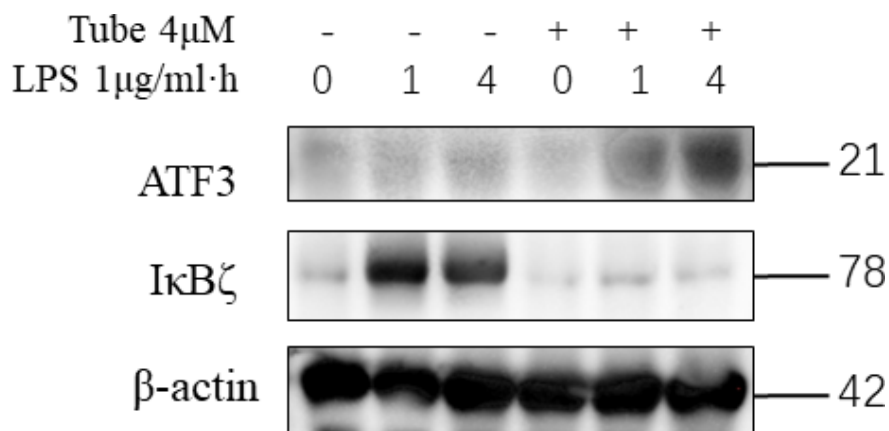


Figure 13. Effect of Tube on ATF3 and IκBζ protein levels

3.9 Itaconic acid inhibitor citraconate reverses the anti-inflammatory effect of Tube

The spleen in the model group was significantly more congested, darker in color, and blunted at the rim than the control group, suggesting splenic hyperfunction of the spleen LPS induction (**Figure 14**). Compared with the model group, the Tube group showed less spleen congestion and relatively lighter color; the overall appearance was similar to that of the control group. Splenic congestion in the inhibitor group was similar to that in the model group and more pronounced than in the Tube group, suggesting that the inhibitor citraconate reduced the protective effect of Tube on the spleen.

RT-PCR experiments showed that IL-1β, IL-6, and iNOS mRNA expression levels were significantly lower in the Tube group than the LPS group, suggesting that Tube inhibited the transcription of IL-1β, IL-6 and iNOS mRNA (**Figure 15**). IL-1β and IL-6 mRNA levels were higher after the use of itaconic acid inhibitor citraconate in the Tube+ inhibitor group compared with the Tube group, suggesting that citraconate decreases the inhibitory effect of Tube on inflammatory factor transcription.

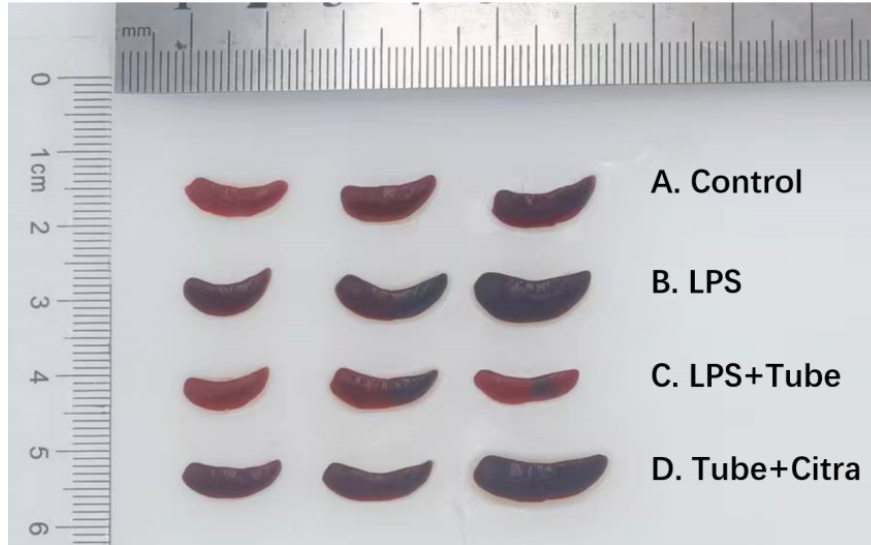
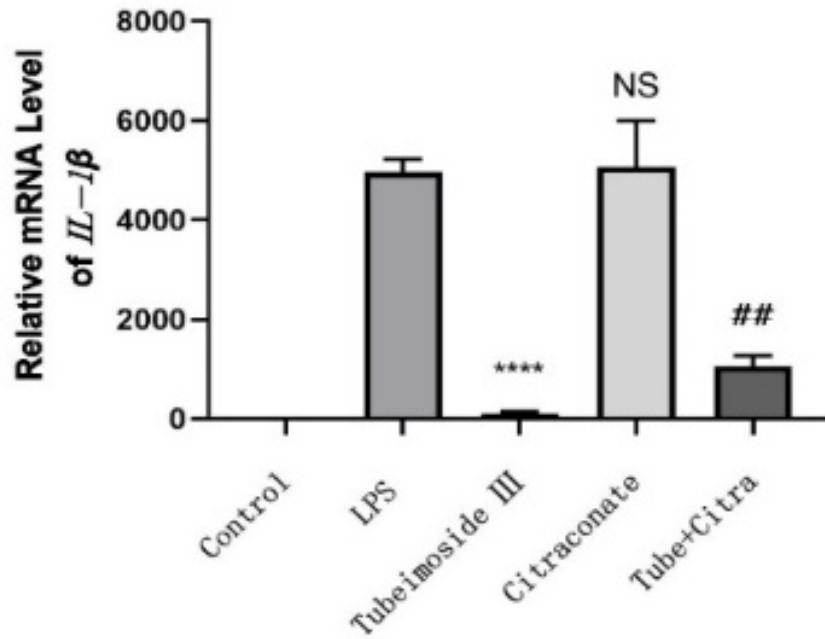


Figure 14 . (A) The control group was injected with an equal amount of sterile PBS intraperitoneally. (B) The LPS group was the model group, and 10 mg/kg LPS solution was injected intraperitoneally. (C) The LPS+Tube group was the Tube group treated with 10 mg/kg LPS solution for 3 hours after intraperitoneal injection of 1 mg/kg Tube. (D) The Tube+Citra group was the inhibitor group, with an intraperitoneal injection of citraconate and Tube, followed by 10 mg/kg LPS solution after 3 hours.



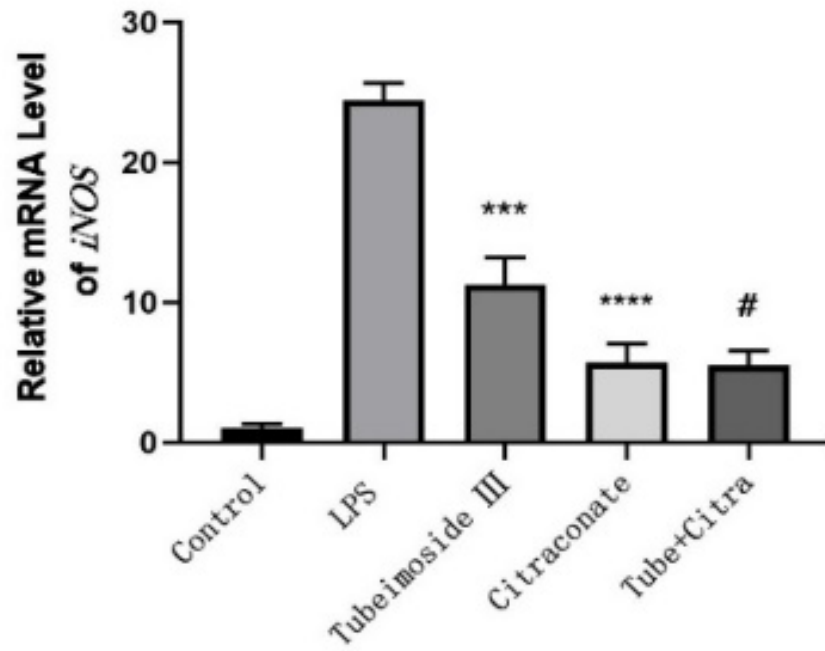
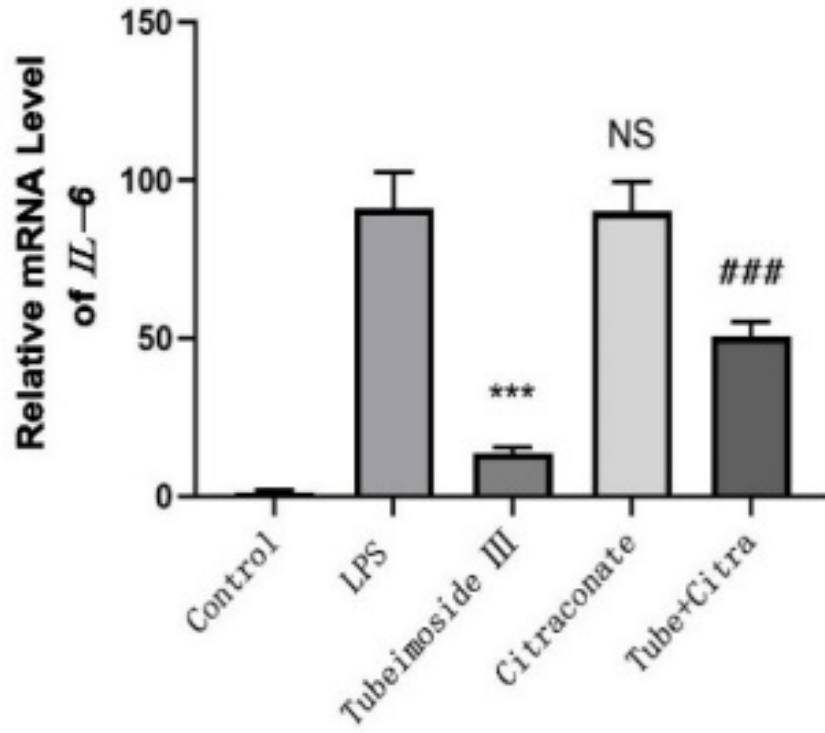


Figure 15. Control: blank control group; LPS: LPS group; Tubimoside III: Tube group; Citraconate: inhibitor group; Tube+Citra: Tube+inhibitor group. ***P < 0.001, ****P < 0.0001 VS LPS. ##P < 0.01, ###P < 0.001 vs. Tube. Values are expressed as mean \pm SEM, and each experiment was repeated three times.

4 Discussion

NO, IL-1 β , IL-6, and TNF- α participate in the pathogenesis of inflammatory diseases[13, 14]. We found that Tube inhibited the expression of IL-1 β , IL-6, and iNOS and suppressed NO production but did not affect TNF- α expression in LPS-induced RAW264.7 cells. We also measured NF- κ B and MAPK signaling pathway-related proteins (e.g., NF- κ B p65 and MAPK p38) and found that Tube had no significant effect on the phosphorylation levels[15-20]. These findings suggest that Tube may not inhibit inflammation through the classical NF- κ B signaling pathway. Small molecules of bacterial origin can be recognized by cell surface receptors and activate relevant signal transduction, leading to the reprogramming of macrophage energy metabolism from mitochondrial oxidative phosphorylation to a high rate aerobic glycolysis; this reprogramming regulates the synthesis and accumulation of macrophage immune metabolites, which in turn affects the expression of inflammatory factors.

Glucose transporter protein (GLUT1) and lactate dehydrogenase (LDH) play pivotal roles in glycolysis. They convert glucose into pyruvate and lactate, which then enter the tricarboxylic acid (TCA)[21, 22]. Tube increased the mRNA levels of fructose-2,6-bisphosphatase 3, HK2, and GLUT1, the rate-limiting enzyme genes of glycolysis, but decreased mRNA levels of LDH. These findings suggest that Tube causes cellular accumulation of pyruvate; therefore, we measured the pyruvate content in RAW264.7 cells and found that Tube did increase it. Notably, we found little effect of Tube on basal and maximal respiration in RAW264.7 cells; therefore, we tentatively concluded that Tube increases the production of pyruvate, an intermediate product of glycolysis, and does not increase levels of mitochondrial oxidative respiration. Pyruvate is involved in energy metabolism by entering the TCA cycle; therefore, Tube might exert its anti-inflammatory effect by regulating the energy metabolic process.

Macrophage metabolic pathways are altered during inflammatory responses, known as “metabolic reprogramming”[23]. We found that metabolic reprogramming participates in the development of inflammatory responses by regulating the expression of macrophage inflammatory factors[24]. Moreover, we observed an intermediate product, itaconic acid. During LPS stimulation, macrophages upregulate expression of immune response gene 1, a mitochondria-related enzyme that catalyzes the conversion of cis-aconitate into itaconate and inhibits succinate dehydrogenase through competitive binding, creating a metabolic breakpoint in the TCA cycle and blocks the TCA cycle[17, 25]. Itaconic acid inhibits the electron transport chain in mitochondria[25, 26], and it regulates the transcription of IL-1 β and IL-6 through the ATF3-I κ B ζ axis; however, it has no significant effect on the transcription level of TNF- α [8, 10]. Τηρερεφορε, ωε μεασυρεδ εξπρεσσιον λεελς οφ δωωνστρεαμ εφφερεστορ μολεσυλες οφ ιτασονικ ασιδ υσινγ PT-ITP εξπεριμεντες ανδ φουνδ τηατ Τυβε ωασ ασσοσιατεδ ωιτη τηε ρεγυλατορψ ρολε οφ ιτασονικ ασιδ.

I κ B ζ is a transcriptional regulator of the non-classical NF- κ B signaling pathway. It binds to the NF- κ B p50 subunit and promotes the transcription of pro-inflammatory factors, including IL-6, IL-1 β , and IL-1 α [27, 28]. Ελεετροπηλικις στρεεσ ινδυσεδ βψ ιτασονικ ασιδ ινηβιτεδ I κ B ζ by upregulating activating transcription factor 3 (ATF3), reducing the production of the pro-inflammatory factor IL-6[8]. Western blot showed that Tube increased the ATF3 protein level and inhibited I κ B ζ protein levels. These findings suggest that Tube exerts its anti-inflammatory effect by reprogramming glucose metabolism in macrophages, affecting the metabolism of the small molecule itaconic acid. Finally, to confirm the necessity of the anti-inflammatory effect of itaconic acid on Tube, we used an inhibitor of itaconic acid, citraconate (that competitively inhibits aconitate decarboxylase 1)[29]. Citraconate impaired the protective effect of Tube in the LPS-induced acute inflammation model. Citraconate also attenuated the downregulation of IL-1 β and IL-6 by Tube. These results suggest that Tube requires the involvement of itaconic acid to exert its inflammatory inhibitory effects.

In summary, tubeimoside III regulates the reprogramming of macrophage glucose metabolism, increasing the content of small metabolic molecule itaconic acid, inhibiting the expression of IL-1 β , IL-6, and iNOS, and reducing the inflammatory response.

Acknowledgments

This work was supported by the National Natural Science Foundation of China (Grant numbers 81760332), the Tibet Natural Science Foundation (Grant numbers XZ202101ZR0100G), the Research Found for Advanced Talents of Xizang Minzu University (Grant numbers RCYJ602111), National Natural Science Foundation of China, Medical School of Xizang University for Nationalities (Grant numbers XZMZ-M2022N02), National University Students Innovation Research Project (Grant numbers 202010695029 and 202110695033) and Graduate research innovation and Practice project of Xizang Minzu University (Grant numbers Y2022097). Key Laboratory for Molecular Genetic Mechanisms and Intervention Research on High Altitude Disease of Tibet Autonomous Region (Grant numbers KF2022008).

References

1. Mitchell JP, Carmody RJ: **NF- κ B and the Transcriptional Control of Inflammation** . *Int Rev Cell Mol Biol* 2018,**335** :41-84.
2. Gilmore TD: **Introduction to NF-kappaB: players, pathways, perspectives** . *Oncogene* 2006, **25** (51):6680-6684.
3. Commission CP: **Pharmacopoeia of the People's Republic of China 2020 Edition** . Beijing: China Pharmaceutical Science and Technology Press; 2020.
4. Li H, Wu KX, Shi KH, Tang L, Liang CY: **Research progress on chemical constituents, pharmacological activities and clinical application of *Bolbostemma paniculatum*** . *China Journal of Chinese Materia Medica* 2021, **46** (17):4314-4322.
5. Yu L, Yu T, Ma R: **Inhibition of the tumor promoting action of 12-O-tetradecanoylphorbol-13-acetate by tubeimoside III isolated from *Bolbostemma paniculatum*** . *Carcinogenesis* 1995,**16** (12):3045-3048.
6. Yu TX, Ma RD, Yu LJ: **Structure-activity relationship of tubeimosides in anti-inflammatory, antitumor, and antitumor-promoting effects** . *Acta Pharmacol Sin* 2001, **22** (5):463-468.
7. Inamdar S, Tylek T, Thumsi A, Suresh AP, Jaggarapu M, Halim M, Mantri S, Esrafil A, Ng ND, Schmitzer E *et al* : **Biomaterial mediated simultaneous delivery of spermine and alpha ketoglutarate modulate metabolism and innate immune cell phenotype in sepsis mouse models** . *Biomaterials* 2023, **293** :121973.
8. Bambouskova M, Gorvel L, Lampropoulou V, Sergushichev A, Loginicheva E, Johnson K, Korenfeld D, Mathyer ME, Kim H, Huang LH *et al* : **Ελεστροπηλις προπερτιες οφ ιτασονατε ανδ δεριατιες ρεγυλατε της Ικβζ-ΑΤΦ3 ινφλαμματορψ αξις** . *Nature* 2018,**556** (7702):501-504.
9. Runtsch MC, Angiari S, Hooftman A, Wadhwa R, Zhang Y, Zheng Y, Spina JS, Ruzek MC, Argiriadi MA, McGettrick AF *et al* : **Itaconate and itaconate derivatives target JAK1 to suppress alternative activation of macrophages** . *Cell Metab* 2022,**34** (3):487-501.e488.
10. Chen LL, Morcelle C, Cheng ZL, Chen X, Xu Y, Gao Y, Song J, Li Z, Smith MD, Shi M *et al* : **Itaconate inhibits TET DNA dioxygenases to dampen inflammatory responses** . *Nat Cell Biol* 2022, **24** (3):353-363.
11. Mills EL, Ryan DG, Prag HA, Dikovskaya D, Menon D, Zaslona Z, Jedrychowski MP, Costa ASH, Higgins M, Hams E *et al* : **Itaconate is an anti-inflammatory metabolite that activates Nrf2 via alkylation of KEAP1** . *Nature* 2018,**556** (7699):113-117.

26. Sun KA, Li Y, Meliton AY, Woods PS, Kimmig LM, Cetin-Atalay R, Hamanaka RB, Mutlu GM: **Endogenous itaconate is not required for particulate matter-induced NRF2 expression or inflammatory response** .*Elife* 2020, **9** .
27. Gautam P, Maenner S, Cailotto F, Reboul P, Labialle S, Jouzeau JY, Bourgaud F, Moulin D: **Εμεργινγ ρολε οφ ΙκΒζ ιν ινφλαμματιον: Εμπηασις ον ποσοριασις** . *Clin Transl Med* 2022,**12** (10):e1032.
28. Trinh DV, Zhu N, Farhang G, Kim BJ, Huxford T: **The nuclear I kappaB protein I kappaB zeta specifically binds NF-kappaB p50 homodimers and forms a ternary complex on kappaB DNA** . *J Mol Biol* 2008,**379** (1):122-135.
29. Chen F, Elgaher WAM, Winterhoff M, Büssov K, Waqas FH, Graner E, Pires-Afonso Y, Casares Perez L, de la Vega L, Sahini N *et al* :**Citraconate inhibits ACOD1 (IRG1) catalysis, reduces interferon responses and oxidative stress, and modulates inflammation and cell metabolism** . *Nat Metab* 2022, **4** (5):534-546.